EFFECTIVE PROPERTIES OF RESONANT NANOPARTICLE SUSPENSIONS: IMPACT OF THE ELEMENTARY VOLUME SHAPE

Timothee Guerra, Inigo Gonzalez de Arrieta, Olivier Rozenbaum, Cédric Blanchard

EFFECTIVE PROPERTIES OF RESONANT NANOPARTICLE SUSPENSIONS: IMPACT OF THE ELEMENTARY VOLUME SHAPE

Timothée Guerra[1], Iñigo González de Arrieta[1,2], Olivier Rozenbaum[1], Cédric Blanchard[1*]

[1]CNRS, CEMHTI UPR3079, Univ. Orléans, Orléans F-45071, France
[2]Physics Department, University of the Basque Country (UPV/EHU), Leioa E-48940, Spain

ABSTRACT. This paper is concerned with the homogenization of nanoparticle suspensions when resonant behaviors are involved, leading to unusual results, such as high incoherence or scattering. At first glance, this seems incompatible with homogenization, which only applies to the coherent part of the electromagnetic response of the suspension. Homogenization procedures must be based on averaging the response of many statistical samples of the suspension, characterized by their size and shape. The focus is on the effect of the agglomerate shape, which is explored by considering elliptical samples of the suspension of different aspect ratio; a section is devoted to the problem of scattering by an ellipse. We show that incoherence is not an intrinsic characteristic of a medium, but a function of its shape. Hence, it is possible to go from a restricted to an unrestricted homogenization just by changing the shape, which does not affect the resulting effective refractive index.

1. INTRODUCTION

In a context of global warming, the development of innovative materials for improving the performance of renewable energy sources is an acute need. An important family among these is that of heterogeneous materials composed of nanoparticles, with structures that allow for the tuning of optical properties [1,2]. One such example is the use of nanoparticles deposited on solar cells to increase absorption [3]. Numerical simulations offer the possibility of exploring how these optical properties relate to the refractive indices and textural properties (arrangement, concentration and size) of the heterogeneities.

However, representative simulations of random materials can only be obtained by sampling a representative volume element (RVE). The exact resolution of Maxwell's equations for these systems can quickly become very expensive in terms of time and computer resources. In order to circumvent this issue, it is common to homogenize the heterogeneous medium and then work with the effective properties. Usually, effective medium theories (EMTs), such as Maxwell-Garnett [4] or Bruggeman [5], are used to compute an effective refractive index for an idealized homogeneous equivalent to the heterogeneous sample. However, these approximations are quite limited in scope, and a more sophisticated homogenization procedure is needed in general. Our motivation in this paper is to explore cases where even a sophisticated method is tested to its limits, to figure out if homogenization is even possible in such instances.

The paper is structured as follows. Section 2 is devoted to a discussion on the link between radiative transfer and homogenization, along with important concepts of homogenization, such as the coherent and incoherent parts of the field. A summary of the homogenization procedure is made afterwards. In

* Corresponding Author: cedric.blanchard@cnrs-orleans.fr.

Section 3, we briefly develop the theory of light scattering by a homogeneous ellipse, i.e., the shape we chose for the evaluation of the sampled volume elements. Finally, Section 4 details the results of homogenization of nanoparticle ensembles in challenging situations, where either incoherence or scattering are high. We show that incoherence is not an intrinsic characteristic of a medium, but a function of its shape. Hence, it is possible to go from a restricted to an unrestricted homogenization just by changing the shape, which does not affect the resulting effective refractive index.

2. RADIATIVE TRANSFER AND HOMOGENIZATION

In order to describe radiative transfer in materials, approximate solutions to the Radiative Transfer Equation (RTE) are often employed. In the transport approximation, for example, the solution is constructed as a function of the transport scattering coefficient σ_{tr} and the transport extinction coefficient β_{tr}, the difference between the two being the absorption coefficient α [6]. In the independent scattering regime, where the interaction between particles can be disregarded, these three phenomena can be related to the single-particle cross-sections and the density of the heterogeneities [7]. However, for non-negligible inter-particle interactions, the so-called dependent scattering regime, the direct computation of the coefficients in the general case is still an open question. For the particular case where the considered medium is homogenizable, that is, when an effective refractive index n_{eff} describing its electromagnetic behavior can be computed, the following extinction coefficient can be computed [8]:

$$K_{ext} = \frac{4\pi}{\lambda} Im(n_{eff}). \tag{1}$$

For an inhomogeneous medium to be unrestrictedly homogenizable, it needs to be composed of non-resonant scatterers that are smaller than the wavelength [9,10]. In these circumstances, the most common EMTs can be applicable. However, these theories are incapable of describing certain situations, such as resonant nanoparticle suspensions [11]. Moreover, if the size of the scatterers is non-negligible, then scattering inside the medium emerges [12] and homogenization becomes restricted [13]. A restricted homogenization means that the effective refractive index only describes a part of the general electromagnetic response: the coherent component. The part that cannot be accounted for by an effective index is called the incoherent part. The coherent-to-incoherent ratio tends to decrease with the size of the individual scatterers. Therefore, one can consider that the concept of homogenization stops making sense whenever this ratio is below a certain threshold, as it only describes a negligible part of the general electromagnetic response. However, the particle size is not the only criterion that leads to restricted homogenization; it can be so even if scatterers are very small compared to the wavelength, whenever resonant interactions are found in the medium [9,11].

Let us consider an inhomogeneous medium that is homogenizable, meaning it is possible to find an index n_{eff} that describes its coherent electromagnetic behavior. To do that, one can take a finite sample of the macroscopic medium and calculate the refractive index that a homogeneous equivalent would need to possess to produce the same electromagnetic response. Because only a finite sample was evaluated, its effective index will deviate by an amount δn_{eff} from the exact value. Accordingly, the electromagnetic behavior of this sample can be split into a mean component and a fluctuating one:

$$\begin{cases} \boldsymbol{E}(\boldsymbol{r}) = \langle \boldsymbol{E} \rangle(\boldsymbol{r}) + \boldsymbol{\delta E}(\boldsymbol{r}), \\ \boldsymbol{H}(\boldsymbol{r}) = \langle \boldsymbol{H} \rangle(\boldsymbol{r}) + \boldsymbol{\delta H}(\boldsymbol{r}), \end{cases} \tag{2}$$

where $\boldsymbol{E}$ and $\boldsymbol{H}$ are the electric and magnetic fields, respectively; $\langle \cdot \rangle$ is the mean field arising from n_{eff} and $\delta \cdot$ the fluctuating part due to δn_{eff}. By definition, $\langle \delta \vec{E} \rangle = \langle \delta \vec{H} \rangle = 0$. Thus, in order to get rid of

the fluctuating part and extract the accurate value of n_{eff}, it is clear from Eq. (2) that we need to consider averages of the physical quantities of interest over a sufficient number of configurations or statistical samples of the medium.

In practice, we generate and simulate the electromagnetic response of a great number of configurations of a very large randomly generated texture with a certain filling factor f. Each configuration will sample a certain portion of the space, with a particular spatial arrangement of the scatterers. The simulation is carried out by a direct method via the use of the multiple-sphere T-matrix method [14,15]. In short, this allows the exact computation of the response of all the scatterers of the agglomerate to an incoming field by taking into account the multiple scattering between particles. Multiple scattering is accounted for via the use of the *addition theorem*, which links together multipolar expansions of the fields in the coordinate systems of each particle [16,17]. As a result, we have access to the scattered fields of each configuration ($\boldsymbol{E_{sc}}$ and $\boldsymbol{H_{sc}}$). It is then possible to compute the mean total Poynting vector using:

$$\langle \boldsymbol{S_{tot}} \rangle = \frac{1}{2} Re(\langle \boldsymbol{E_{sc}} \times \boldsymbol{H_{sc}^*} \rangle), \tag{3}$$

where $\cdot^*$ stands for the complex conjugate. Using the definition of the fields given in Eq. (2), Eq. (3) can be rewritten into:

$$\langle \boldsymbol{S_{tot}} \rangle = \frac{1}{2} Re(\langle \boldsymbol{E_{sc}} \rangle \times \langle \boldsymbol{H_{sc}^*} \rangle) + \frac{1}{2} Re(\langle \boldsymbol{\delta E_{sc}} \times \boldsymbol{\delta H_{sc}} \rangle), \tag{4}$$

where the first term corresponds to the coherent part of the Poynting vector ($\boldsymbol{S_{soh}}$) and the second to its incoherent part ($\boldsymbol{S_{incoh}}$).

Using these quantities, the exact procedure for homogenization is as follows:

- Compute $\boldsymbol{S_{coh}}$ of the inhomogeneous medium.
- Compute the Poynting vector ($\boldsymbol{S_{hom}}$) of an homogeneous medium with refractive index n_{hom}.
- Fit $\boldsymbol{S_{hom}}$ to $\boldsymbol{S_{coh}}$. When the match between the two is satisfactory, then $n_{eff} = n_{hom}$.

For this procedure to be accurate, the number of configurations is a crucial parameter. Taking too few may lead to a badly defined coherent part, which results in a poor extraction procedure. On the other hand, too many configurations lead to intractable simulation times. The other important parameter to consider in these simulations is the size of each configuration; it needs to be a RVE of the medium [18,19]. If it is too small, then the interactions between particles inside each configuration might not be representative of the typical interactions found in the global medium, which will introduce a bias in the obtained value for n_{eff}.

To the best of our knowledge, the shape of the individual configurations has not been studied as a significant parameter for homogenization. Spherical samples are usually considered [10,11,20,21], as the fitting procedure can rely on the well-established Mie theory for the equivalent homogeneous sphere [22]. The goal of this article is to test whether using other shapes has an effect on the procedure and the obtained results, by comparing the results obtained for elliptical samples to those of circular ones. The study was conducted using 2D media to avoid the computational burden that would be required for a 3D study.

3. LIGHT SCATTERING BY A HOMOGENEOUS ELLIPSE

Light scattering by an elliptical particle is less known compared to light scattering by a circular particle for which many textbooks exist [23,24]. Therefore, let us first derive the equations that we are going to need before examining the homogenization results. Starting from the Helmholtz equation, it was demonstrated that it is possible to use the separation of variable to solve it in elliptic coordinates [25]. Let us define the electric field as $E(\xi,\eta) = f(\xi)g(\eta)$, where ξ and η are the elliptical coordinates. By inserting this separation in the Helmholtz equation, one can derive the two following equations:

$$\begin{cases} \dfrac{\partial^2 g}{\partial \eta^2} + [\lambda - 2q\cos(2\eta)]g(\eta) = 0, \\ \dfrac{\partial^2 f}{\partial \xi^2} + [\lambda - 2q\cosh(2\xi)]f(\xi) = 0, \end{cases} \tag{5}$$

where λ is the characteristic value and q the Mathieu parameter. In our case, q is linked to the wave number k and the eccentricity c of the ellipse via $4q = (kc)^2$. From onwards, we use the notation of Abramowitz [26] and Meixner [27], alongside with their normalization. The solutions of Eq. (5) first line are called angular Mathieu functions and are given by Eq. (20.2.3) and Eq. (20.2.4) of [26], whereas the solutions of Eq. (5) second line are called radial Mathieu functions and are given by Eq. (20.6.7-20.6.10) of [27].

Now let us consider a plane wave with wavelength λ and temporal dependence $e^{-i\omega t}$ traveling inside a medium with refractive index n_m (often considered as vacuum) impinging on an ellipse with major axis a, minor axis b and refractive index n_e at an angle θ_0 from the x-axis. The magnetic field is parallel to the z-axis, transverse–magnetic (TM) polarization, whereas the direction of propagation is perpendicular to it, so:

$$H_z^{inc}(x,y) = H_0 e^{-ik_m(x\cos\theta_0 + y\sin\theta_0)}, \tag{6}$$

where $k_m = 2\pi n_m/\lambda$ is the wavenumber in the host medium and H_0 the amplitude of the incident wave. Following Meixner's approach, such a plane wave can be decomposed into the sum of Mathieu functions as follows [27]:

$$H_z^{inc}(\xi,\eta) = H_0 \sum_{n=-\infty}^{+\infty} (-i)^n me_n(-\theta_0, q_m) Me_n^{(1)}(\xi, q_m) me_n(\eta, q_m), \tag{7}$$

where me_n is the angular Mathieu function of order n and $Me_n^{(1)}$ is the first radial Mathieu function of order n. Upon interaction of the incident wave on the ellipse, an outgoing scattered field is emitted, which can be represented using the elliptical traveling wave function $Me_n^{(3)}$. Inside the ellipse, the field can be represented with the same kind of expression as the incident field, except for the substitution $q_m \rightarrow q_e$:

$$\begin{cases} H_z^{sca}(\xi,\eta) = H_0 \displaystyle\sum_{n=-\infty}^{+\infty} b_n Me_n^{(3)}(\xi, q_m) me_n(\eta, q_m), \\ H_z^{int}(\xi,\eta) = H_0 \displaystyle\sum_{n=-\infty}^{+\infty} c_n Me_n^{(1)}(\xi, q_e) me_n(\eta, q_e), \end{cases} \tag{8}$$

where b_n and c_n are the scattering and interior coefficients to be determined, respectively. The radial and tangential fields can be computed using [25]:

$$\begin{cases} E_\xi = \dfrac{1}{i\omega\epsilon}\dfrac{1}{\sqrt{\cosh^2\xi - \cos^2\eta}}\dfrac{\partial}{\partial\eta}\left(\dfrac{H_z}{c}\right), \\ E_\eta = -\dfrac{1}{i\omega\epsilon}\dfrac{1}{\sqrt{\cosh^2\xi - \cos^2\eta}}\dfrac{\partial}{\partial\xi}\left(\dfrac{H_z}{c}\right), \end{cases} \tag{9}$$

where ϵ can either be the permittivity of the medium ϵ_m or the ellipse ϵ_e. Imposing the usual continuity condition of the axial and tangential components at the interface of the ellipse - defined by $\xi = \xi_0 = \frac{1}{2} ln\left(\frac{a+b}{a-b}\right)$ -, it is possible to compute the coefficients b_n and c_n. Using the asymptotic expression of the modified Mathieu functions $Me_n^{(3)}$ given in [28], the final expression of the far-field flux scattered by the ellipse is obtained after some more algebra that is not reproduced here for the sake of space, and is given by the following expansion:

$$F(\eta) = \frac{2}{\pi k_m}\left|\sum_{n=-\infty}^{+\infty}(-i)^n b_n me_n(\eta, q_m)\right|^2 . \tag{10}$$

The goal of the homogenization procedure will be to compare $\|\boldsymbol{S_{coh}}\|$ to $F(\eta)$ to obtain the effective refractive index.

4. HOMOGENIZATION OF RESONANT INTERACTING NANOPARTICLES

Let us consider a medium made of nanoparticles, with a radius $r_p = 100$ nm and complex refractive index n. These nanoparticles are randomly distributed with a filling factor $f_p = 15\%$ inside a boundary whose shape can be a circle with radius R_a or an ellipse with major and minor axis defined as $A = R_a\sqrt{\tau}$ and $B = R_a/\sqrt{\tau}$, respectively, where $\tau = A/B$. This definition ensures that the ellipse and the circle have the same surface and thus the same number of particles inside. Some examples of ellipses with $R_a = 5$ μm and different τ are represented in Figure 1(a). All averages will be taken over 1000 configurations with the same τ value. Each agglomerate of nanoparticles is illuminated by a plane wave with TM polarization and wavelength $\lambda = 10$ μm.

In a previous article [9], we found that homogenization was challenging for the following particle refractive indices: $n_1 = 0.029 + 1.732i$ and $n_2 = 0.044 + 1.129i$. The first case corresponds to a regime where incoherence is high, a situation in which homogenization is by definition restricted. However, unlike the common belief that incoherence is an indicator of scattering in the medium [13], scattering was found to be negligible in this case. On the contrary, little incoherence and strong scattering were found in the second case, which also renders homogenization questionable, as a homogeneous medium should not present internal scattering. Furthermore, this case requires a very large RVE, rendering simulations cumbersome [19].

Figures 1(b)/(c) display the ratio of incoherence to mean flux as a function of R_a for different τ for refractive indices n_1 and n_2, respectively. The expectation is that all configurations would become more similar with an increase in the agglomerate radius, thus leading to a reduced incoherent response (i.e., $\lim_{R_a\to\infty}\langle\delta\vec{E}\rangle = 0$). This is indeed the case for the simulations carried out with n_2, as shown in Figure 1(c). However, it is possible to find cases for which the incoherence does not have a stable behavior, but

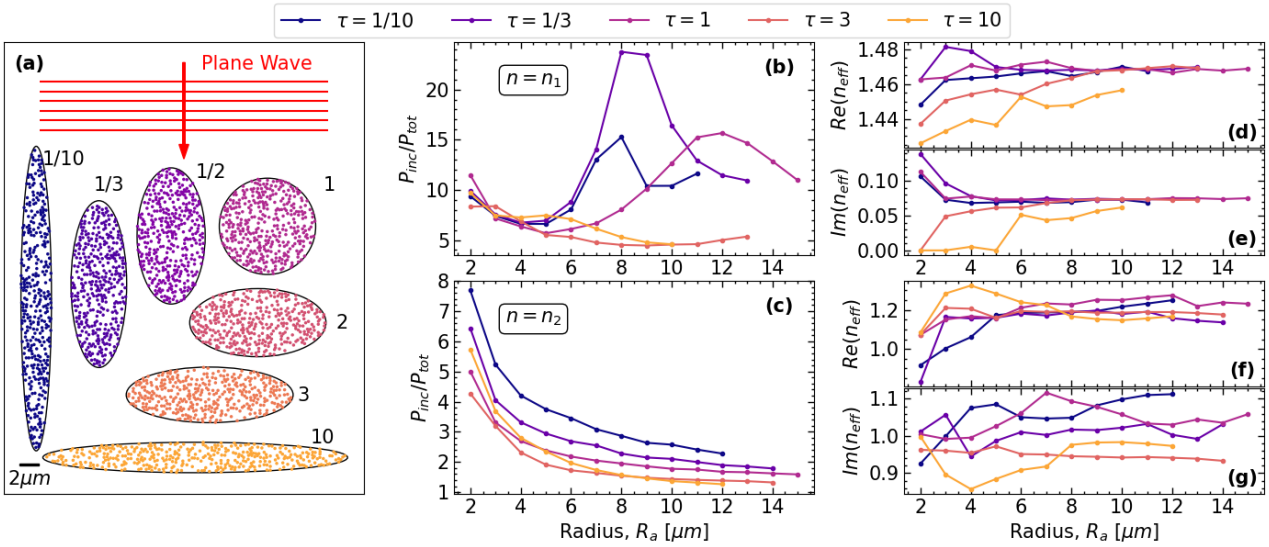

Figure 1. (a) Examples of ellipses with $R_a = 5$ μm, where each shape is labeled by its τ value. (b) Ratio of incoherence to mean flux as a function of R_a for different τ for calculations made with $n = n_1$. (c) Same as (b), but for $n = n_2$. (d)/(e) Real/imaginary parts of the effective refractive index as a function of R_a for different τ for $n = n_1$. (f)/(g) Same figure, but for $n = n_2$.

oscillates with the radius, as in Figure 1(b). What is more, this strange behavior is observed for all values of τ . Whereas the oscillations for $\tau > 1$ (main axis perpendicular to the propagation) seem attenuated, this is not the case for circular configurations or ellipses with $\tau < 1$. This means that incoherence is not an intrinsic characteristic of a medium, as it is possible to increase or reduce its amount just by changing the shape of the configurations.

Regarding the numerical results of the homogenization procedure, Figures 1(d,e) display the real and imaginary parts of the effective refractive indices obtained for $n = n_1$ as a function of R_a, for different τ. By increasing R_a, a clear convergence towards a single value is observed, irrespective of τ. This is a clear illustration of the concept of RVE: the larger the configuration, the more representative it is of the medium, and therefore the better the homogenization. In addition, this proves that homogenization using elliptical configurations is possible and agrees well with the result obtained with a circular shape ($\tau = 1$). Interestingly, homogenization with moderate incoherence ($\tau = 3$) gives the same results as homogenization with higher incoherence ($\tau < 1$). Note that in the first case, the homogenization can be considered unrestricted, whereas in the second case, it is restricted. This implies that the quality of homogenization is independent of the amount of incoherence. This result runs opposite to the widely held assumption that high incoherence implies that homogenization is not possible.

The extraction of the real/imaginary parts of n_{eff} from $n = n_2$ is displayed in Figures 1(f)/(g). The homogenization does not converge towards a single value, but strongly depends on τ. This is especially true for the imaginary part. To get more insight into this particular case, the coherent and incoherent scattering far-field flux diagram for configurations with $R_a = 12$ μm are represented in Figure 2, as a function of τ. It seems that the fit for $\tau = 1/10$ is not able to successfully reproduce the back-scattered radiation. In contrast, for $\tau = 10$, it is the radiation scattered perpendicular to the forward direction which is underestimated. These results suggest that the homogenization for these two cases is probably less trustworthy than the others tested τ. However, for the three other cases, the fit matches perfectly the coherent flux. Therefore, in the absence of any other indicator, it is not possible to discriminate which of these values, if any, is the true one. Most probably, the RVE is still bigger than the tested agglomerate

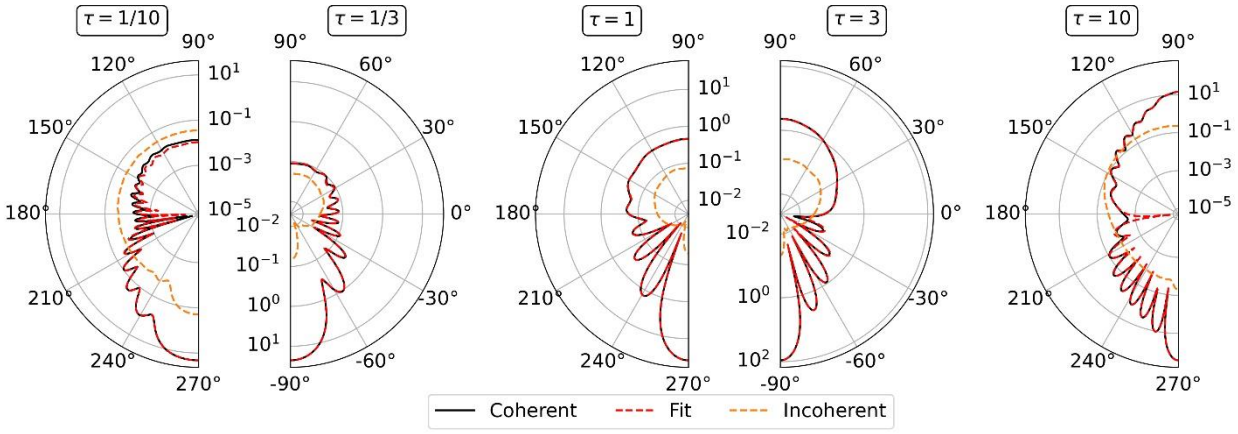

Figure 2. Scattering far-field flux diagram for $n = n_2$ and $R_a = 12$ µm, as a function of angle and eccentricity (τ). The radial axis is in logarithmic scale. Only half of the polar angles are shown, as the diagrams are almost perfectly symmetric.

radius, implying that the extraction procedure, as implemented in this work, is still biased. For computation reasons, we were not able to pursue the investigation further.

5. CONCLUSIONS

To homogenize a heterogeneous medium made of interacting nanoparticles, one can compare the coherent far-field flux of a number of configurations to the far-field flux of a homogeneous equivalent; by matching the two, the effective refractive index can be retrieved. The three main parameters for such procedure are the number, the size and the shape of the configurations. The first two were already extensively studied and are linked to the concept of RVE. In this paper, we investigated the impact of the shape of individual configuration on the homogenization by comparing the effective refractive index obtained with ellipses and circles.

After having summarized the scattering theory for ellipses, we have shown that the shape can have a great impact on the amount of incoherence, implying that the incoherent field is not necessarily an intrinsic characteristic of the medium. For the same medium, we were able to go from a restricted homogenization with high incoherence to an unrestricted homogenization with little incoherence just by changing the shape. In both cases, the obtained effective refractive indices are the same.

Finally, we investigated a case that was demonstrated to exhibit high scattering alongside a large RVE, making the homogenization challenging and rendering simulations complex. Changing the shape turned out to lead to different solutions for the effective refractive index. However, in the absence of a clear indicator of which solution is the exact one, it was impossible to discriminate them.

ACKNOWLEDGEMENTS

We acknowledge financial support from the French National Research Agency (ANR) as part of the "Jeunes Chercheuses et Jeunes Chercheurs" program (project: OUTWARDS, ID: ANR 19-CE05-0021). Iñigo González de Arrieta acknowledges support from the Basque Government by means of a post-doctoral fellowship (POS-2021-2-0022).

REFERENCES

[1] F. Cao, K. McEnaney, G. Chen, Z. Ren, "A review of cermet-based spectrally selective solar absorbers," *Energ. Environ. Sci.*, vol. 7, no. 5, p. 1615, 2014.

[2] A. Urrutia, J. Goicoechea, F. J. Arregui, "Optical Fiber Sensors Based on Nanoparticle-Embedded Coatings," *J. Sens.*, vol. 2015, pp. 1–18, 2015.

[3] K. Nakayama, K. Tanabe, H. A. Atwater, "Plasmonic nanoparticle enhanced light absorption in GaAs solar cells," *Appl. Phys. Lett.*, vol. 93, p. 121904, 2008.

[4] J. C. M. Garnett, "XII. Colours in metal glasses and in metallic films," *Philos. Trans. R. Soc. Lond. Ser. A*, vol. 203, pp. 385–420, 1904.

[5] D. A. G. Bruggeman, "Berechnung verschiedener physikalischer Konstanten von heterogenen Substanzen. I. Dielektrizitätskonstanten und Leitfähigkeiten der Mischkörper aus isotropen Substanzen," *Ann. Phys.-Berlin*, vol. 416, no. 7, pp. 636–664, 1935.

[6] L. A. Dombrovsky, H. K. Tagne, D. Baillis, and L. Gremillard, "Near-infrared radiative properties of porous zirconia ceramics," Infrared Physics & Technology, vol. 51, pp. 44–53, July, 2007.

[7] M. I. Mishchenko, ""Independent" and "dependent" scattering by particles in a multi-particle group," *OSA Continuum*, vol. 1, p. 243, 2018.

[8] S. Durant, O. Calvo-Perez, N. Vukadinovic, J.-J. Greffet, "Light scattering by a random distribution of particles embedded in absorbing media: full-wave Monte Carlo solutions of the extinction coefficient," *J. Opt. Soc. Am. A*, vol. 24, no. 9, p. 2953, 2007.

[9] T. Guerra, D. De Sousa Meneses, J.-P. Hugonin, C. Blanchard, "Unconventional Electromagnetic Response of Strongly Coupled Nanoparticles in the Thermal Infrared Region: Link with Effective Medium Properties and Incoherent Fields," *Part. Part. Syst. Charact.*, vol. 39, p. 2100245, 2022.

[10] M. I. Mishchenko, Z. M. Dlugach, N. T. Zakharova, "Direct demonstration of the concept of unrestricted effective-medium approximation," *Opt. Lett.*, vol. 39, p. 3935, 2014.

[11] C. Blanchard, J.-P. Hugonin, A. Nzie, D. De Sousa Meneses, "Multipolar scattering of subwavelength interacting particles: Extraction of effective properties between transverse and longitudinal optical modes," *Phys. Rev. B*, vol. 102, p. 064209, 2020.

[12] C. F. Bohren, "Applicability of Effective-Medium Theories to problems of Scattering and Absorption by Nonhomogeneous Atmospheric Particles," *J. Atmos. Sci.*, vol. 43, pp. 468–475, 1986.

[13] D.Werdehausen, I. Staude, S. Burger, J. Petschulat, T. Scharf, T. Pertsch, M. Decker, "Design rules for customizable optical materials based on nanocomposites," *Opt. Mater. Express*, vol. 8, p. 3456, 2018.

[14] B. Stout, J.-C. Auger, J. Lafait, "A transfer matrix approach to local field calculations in multiple-scattering problems," *J. Mod. Opt.*, vol. 49, pp. 2129–2152, 2002.

[15] D. Torrent, J. Sánchez-Dehesa, "Effective parameters of clusters of cylinders embedded in a nonviscous fluid or gas," *Phys. Rev. B*, vol. 74, 2006.

[16] S. Stein, "Addition theorems for spherical wave functions," *Q. Appl. Math.*, vol. 19, no. 1, pp. 15–24, 1961.

[17] F. G. Mitri, "Resonance scattering and radiation force calculations for an elastic cylinder using the translational addition theorem for cylindrical wave functions," *AIP Adv.*, vol. 5, p. 097205, 2015.

[18] T. Kanit, S. Forest, I. Galliet, V. Mounoury, D. Jeulin, "Determination of the size of the representative volume element for random composites: statistical and numerical approach," *Int. J. Solids Struct.*, vol. 40, pp. 3647–3679, 2003.

[19] T. Guerra, D. De Sousa Meneses, O. Rozenbaum, C. Blanchard, "From representative volume element of interacting particles to the extraction of their effective properties," *Opt. Express*, vol. 29, p. 35900, 2021.

[20] M. I. Mishchenko, J. M. Dlugach, D. W. Mackowski, "Coherent backscattering by polydisperse discrete random media: exact T-matrix results," *Opt. Lett.*, vol. 36, p. 4350, 2011.

[21] A. Rohfritsch, J.-M. Conoir, R. Marchiano, T. Valier-Brasier, "Numerical simulation of two-dimensional multiple scattering of sound by a large number of circular cylinders," *J. Acoust. Soc. Am.*, vol. 145, pp. 3320–3329, 2019.

[22] G. Mie, "Beiträge zur Optik trüber Medien, speziell kolloidaler Metallösungen," *Ann. Phys.-Berlin*, vol. 330, no. 3, pp. 377–445, 1908.

[23] H. C. van de Hulst, *Light scattering by small particles*, Courier Corporation, 1981.

[24] J. Kong, *Electromagnetic Wave Theory*, Wiley, 1986.

[25] P. H. Moon, D. E. Spencer, *Field theory handbook*, Second Edition, Springer, 1988.

[26] M. Abramowitz, "Handbook of mathematical functions with formulas," In *Graphs, and Mathematical Tables*, National Bureau of Standards, 1965.

[27] J. Meixner, F. W. Schafke, *Mathieusche Funktionen und Sphäroidfunktionen, Grundlehren Der Mathematischen Wissenschaften*, Springer, 1954.

[28] J. Gutiérrez-Vega, "Theory and numerical analysis of the Mathieu functions," 2008.